View metadata, citation and similar papers at core.ac.uk

brought to you by CORE

provided by Tsukuba Repository

Curvature-Induced Metallization of Double-Walled Semiconducting Zigzag Carbon Nanotubes

著者	Okada Susumu, Oshiyama Atsushi
journal or publication title	Physical review letters
volume	91
number	21
page range	216801
year	2003-11
権利	(C)2003 The American Physical Society
URL	http://hdl.handle.net/2241/89417

doi: 10.1103/PhysRevLett.91.216801

Curvature-Induced Metallization of Double-Walled Semiconducting Zigzag Carbon Nanotubes

Susumu Okada and Atsushi Oshiyama

Institute of Physics and Center for Computational Physics, University of Tsukuba, 1-1-1 Tennodai, Tsukuba 305-8571, Japan and Research Consortium for Synthetic Nano-Function Materials Project (SYNAF), National Institute of Advanced Industrial Science and Technology (AIST), 1-1-1 Umezono, Tsukuba 305-8568, Japan

(Received 30 April 2003; published 18 November 2003)

We report total-energy electronic-structure calculations that provide energetics and electronic structures of double-walled carbon nanotubes consisting of semiconducting $(n, 0)$ nanotubes. We find that optimum spacing between the walls of the nanotubes is slightly larger than the interlayer spacing of the graphite. We also find that the electronic structures of the double-walled nanotubes with the inner (7,0) nanotube are metallic with multicarrier characters in which electrons and holes exist on inner and outer nanotubes, respectively. Interwall spacing and curvature difference are found to be essential for the electron states around the Fermi level.

DOI: 10.1103/PhysRevLett.91.216801 PACS numbers: 73.22.–f, 71.20.Tx, 73.20.At

Carbon nanotubes [1] have attracted a lot of attention in the last decade due to possible applications for nanometer scale electronic devices in the next generation [2]. One of the most fascinating characteristics is that the nanotubes exhibit interesting variations of their electronic structures depending on their atomic arrangement along the circumference [3,4]. The electronic structures of the nanotubes are characterized by the chiral index (n, m): The nanotubes are metallic when $|n - m|$ is a multiple of three, whereas they are semiconducting otherwise [3,4]. The peculiar electronic property is originated from anisotropic energy bands of the graphite sheet and an imposed boundary condition in the tubular structure. In addition to the chirality, curvature also affects the electronic structure of the nanotubes. In the graphite, electron states are classified into two groups: σ (sp^2 orbital) and π (p_z orbital) states. In the nanotubes, however, the π states are rehybridized with the σ states due to its lack of mirror symmetry. Thus the rehybridization causes downward shifts of the π electron states of the nanotubes and the amount of the shift depends on the curvature. Indeed, previous theoretical calculations reported that thin $(n, 0)$ nanotubes smaller than (6, 0) become metallic due to the significant π-σ rehybridization [5,6]. Furthermore the curvature also affects the Fermi energy (E_F) of the carbon nanotubes: E_F of the metallic nanotubes indeed depends on their radii [7].

On the other hand, the nanotubes are regarded as natural superunits that could be self-organized to become a unique class of solids with structural hierarchy: Multiwalled nanotubes [1] and bundles of nanotubes [8] are known to be representative examples for such hierarchical structures. The structural hierarchy also modulates the electronic structure of the nanotubes. For the metallic nanotubes, the weak interaction between the nanotubes causes the small band repulsion at E_F and the pseudogap emerges near E_F [9,10].

Recently, high resolution transmission electron microscopy images have shown that ultrathin nanotubes with their diameters of 4–6 Å exist as the innermost shell of the multiwalled nanotubes [11,12]. In addition, thin double-walled nanotubes (DWNTs) are synthesized by using carbon peapods as starting materials [13,14]: Electron beam irradiation on the carbon peapods induces coalescence of encapsulated C_{60}s and results in the DWNTs of which diameters of inner and outer shells are about 6 and 13–14 Å, respectively. Thus the multiwalled nanotubes with thin innermost shells are realistic materials and deserve serious investigation of their electronic structures which are expected to exhibit interesting interplay among the network geometries, the curvature, and the structural multiplicity.

In this Lett, we report total-energy electronic-structure calculations performed for DWNTs consisting of the inner zigzag $(m, 0)$ ($m = 7$, 8, and 10) and the outer $(n, 0)$ ($n = 15$–20) nanotubes. We find that optimum interwall spacing between inner and outer nanotubes is slightly larger than the interlayer spacing of the graphite. We also find that the DWNTs with the $(7, 0)$ inner tube become metallic, while the DWNTs with thicker inner tubes are found to remain semiconducting. It is found that the $(7, 0)$@$(16, 0)$ is a metal in which the conduction and the valence bands merge, giving rise to the finite density of state at the Fermi level. The top of the valence and the bottom of the conduction bands are localized on the outer and inner nanotubes, respectively. Moreover, we find that $(7, 0)$@$(17, 0)$ and $(7, 0)$@$(19, 0)$ nanotubes are semimetals with the electron and hole concentrations of about 1.5×10^{20} cm^{-3}. It is clarified that this surprising electronic structure is due to the significant rehybridization between π and σ states of each nanotube. The manifestation of the effect in other DWNTs is also examined.

All calculations have been performed using the local-density approximation (LDA) in the density-functional

 © 2003 The American Physical Society

theory [15,16]. For the exchange-correlation energy among electrons, we use a functional form [17] fitted to the Monte Carlo results for the homogeneous electron gas [18]. Norm-conserving pseudopotentials generated by using the Troullier-Martins scheme are adopted to describe the electron-ion interaction [19,20]. The valence wave functions are expanded by the plane-wave basis set with a cutoff energy of 50 Ry which is known to give enough convergence of the total energy to discuss the relative stability of various carbon phases [19,21]. We carry out the calculation for double-walled carbon nanotubes, $(7, 0)@(n, 0)$ nanotubes ($15 \leq n \leq 20$), and other DWNTs with different radii. We adopt a supercell model in which a DWNT is placed with its outer wall of the nanotube being separated by 7 Å from the outer wall of an adjacent DWNT. The conjugate-gradient minimization scheme is utilized both for the electronic-structure calculation and for the geometry optimization [22]. In the geometry optimization, we impose a coaxial tube arrangement. Integration over the one-dimensional Brillouin zone is carried out using the eight k points.

First, we explore the stability and the preferable interwall spacing of the DWNTs. Figure 1 shows an energy gain ΔE for the formation of DWNTs $[\Delta E : (7, 0) + (n, 0) \rightarrow (7, 0)@(n, n) - \Delta E]$ as a function of the interwall spacing. It is found that the (16, 0) is the most favorable outer nanotube for the (7, 0) nanotube and gives the largest $|\Delta E|$ of about 0.94 eV/cell with the interwall spacing of 3.52 Å. Moreover, by interpolating the ΔE of zigzag nanotubes calculated here, we estimate that the most preferable interwall spacing for the thin DWNTs is 3.56 Å which is larger than the interlayer spacing of the graphite (3.34 Å). The interlayer spacing determined by the present LDA calculation, 3.35 Å, is slightly larger than the experimental value. The difference between the interlayer and interwall spacings is thus meaningful. The peculiar interwall spacing has been indeed found in the electron diffraction pattern on the DWNTs [23]. It seems that the small tube radius and the incommensurability of atomic arrangements between inner and outer nanotubes causes the larger interwall spacing than the graphite. Since the interwall spacing experimentally observed exhibits substantial distribution around their optimum value [24], the DWNTs other than the most stable $(7, 0)@(16, 0)$ are expected to be synthesized under usual conditions. Thus, we here focus on the most stable two DWNTs, $(7, 0)@(16, 0)$ and $(7, 0)@(17, 0)$, and clarify their electronic structures.

Figures 2(a)–2(c) show electronic structures of zigzag (7, 0), (16, 0), and (17, 0) nanotubes, respectively. As shown in Fig. 2, all the zigzag nanotubes studied here are semiconductors with moderate direct energy gaps at the Γ point. The energy gap of the (7, 0) is narrower than those of the (16, 0) and (17, 0): The calculated values are 0.49, 0.60, and 0.52 eV for (7, 0), (16, 0), and (17, 0), respectively, which are in good agreement with those obtained by the recent GW calculations [25]. The decrease in the energy gap of (7, 0) is a consequence of the fact that the σ-π rehybridization increases with decreasing the tube radius so that the π-like states shift downwards. Therefore, it is expected that the DWNTs consisting of the semiconducting zigzag nanotubes exhibit an interesting variation of electronic structures around the energy gap since the amounts of energy shift of the π and π^* states of the zigzag nanotubes strongly depend on their radii.

The electronic structures of the DWNTs, $(7, 0)@(16, 0)$ and $(7, 0)@(17, 0)$, are shown in Figs. 2(d) and 2(e), respectively, exhibiting surprising features. The energy gap vanishes although each constituent nanotube is a semiconductor with the finite energy gap. In $(7, 0)@(16, 0)$, the π and π^* states merge and thus the density of states at the Fermi level becomes finite due to the characteristics of its one-dimensional energy bands. In $(7, 0)@(17, 0)$, the π and π^* states even overlap and a substantial number of carriers is generated. The formation of the double-walled structures which introduces a new structural multiplicity in the nanotube systems causes the metallization of the semiconductors. Moreover, the results suggest that the multiwalled nanotubes containing the innermost nanotubes with the diameter of 4–6 Å become coated metallic wires. The metallization of the $(7, 0)@(16, 0)$ and the $(7, 0)@(17, 0)$ is totally due to the difference in the downward shift of the π and π^* electron states between the

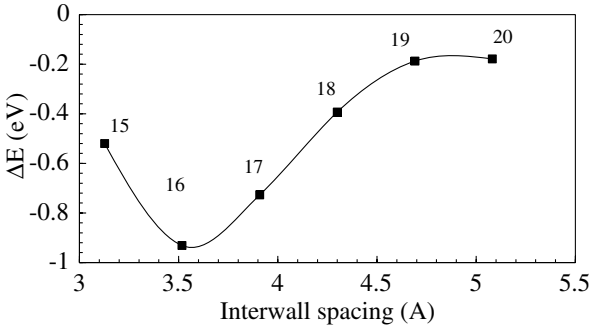

FIG. 1. Energy gain ΔE (see text) per unit cell of the DWNTs $(7, 0)@(n, 0)$, $n = 15$, 16, 17, 18, 19, and 20.

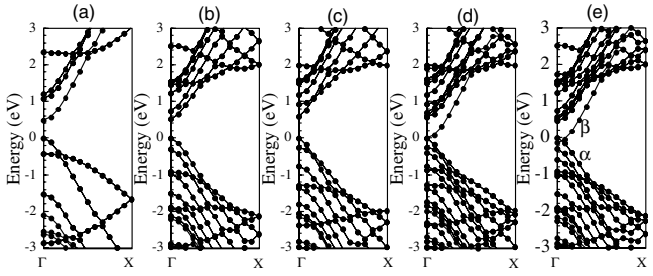

FIG. 2. Energy band structures of (a) (7, 0), (b) (16, 0), (c) (17, 0), (d) $(7, 0)@(16, 0)$, and (e) $(7, 0)@(17, 0)$ nanotubes. Energies are measured from the top of the π band. The α and β denote the electron states of the highest branch of the π band and the lowest branch of the π^* band, respectively.

inner and outer nanotubes: Downward shifts of the π and π^* states of the inner tube are larger than those of the outer tube because of the stronger rehybridization of σ and π states; the bottom of the conduction band possessing the π^* character of the inner nanotube is thus located near or below the top of the valence band distributed on the outer nanotube. Overlap between the conduction band of the inner nanotube and the valence band of the outer nanotube results in the metallization of the DWNTs. Yet it should be mentioned that the many-body correction might be important for the unoccupied energy bands of the semiconducting nanotubes [25] and is to be studied in the future.

The distribution of the wave function unequivocally reveals that the top of the π band (the doubly degenerate α band) is distributed on the outer nanotube while the bottom of the π^* band (the β band) is distributed on the inner nanotube (Fig. 3). In the (7, 0)@(17, 0), it is found that 5% of the α band is unoccupied, whereas 10% of the β band isoccupied. When the (7, 0)@(17, 0) nanotubes are bundled with 3 Å separation, this corresponds to the electron and the hole concentrations of about 1.5×10^{20} cm^{-3}. Thus the DWNTs consisting of the semiconducting nanotubes with thin radius are semimetals in which two kinds of the carriers are isolated in space.

The curvature of the inner tube itself is also an interesting factor to possibly cause the metallization in the DWNTs. We have thus calculated the electronic structures of (8, 0)@(19, 0) and (8, 0)@(20, 0). We have indeed found that downward shifts of conduction and valence bands of the inner tubes relative to those of outer tubes are substantial but that (8, 0) is too thick to cause the metallization: The calculated band gaps for (8, 0)@(19, 0) and (8, 0)@(20, 0) are 0.26 and 0.23 eV, respectively, about half of the gaps of the constituent tubes. The calculations for (10, 0)@(19, 0) and (10, 0)@(20, 0) have been also done, and they are found to be semiconductors with the energy gaps of a half eV. It is thus concluded that the metallization of the DWNTs is a consequence from the subtle balance between the curvature difference of the constituent tubes and the σ-π rehybridization of the inner tube.

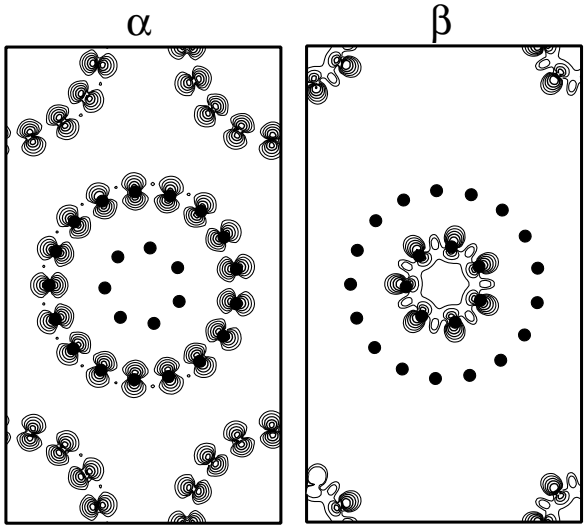

FIG. 3. Contour plots of the squared wave functions at Γ of the highest branch of the π band (α) and the lowest branch of the π^* band (β) on the cross sectional plane of (7, 0)@(17, 0). Each contour represents twice (or half) of the density of the adjacent contour lines. The lowest values represented by the contour is 4.6875×10^{-4} e/(a.u.)^3. The solid circles denote the atomic positions.

The metallization in the DWNTs consisting of constituent semiconducting nanotubes is induced by the curvature difference between the inner (7, 0) and outer nanotubes. Therefore, it is natural to consider that the amount of the band overlap between the π and π^* states monotonically increases with increasing the curvature difference between the inner and outer nanotubes. The situation is not so simple, however. As listed in Table I, the amount of the band overlap for the (7, 0)@(17, 0) is almost the same as those for the (7, 0)@(19, 0) and the (7, 0)@(20, 0), although the curvature difference monotonically increases in the case. The result infers that the space between the nanotubes may affect the electronic structures near the Fermi level of the DWNTs.

The charge redistribution shows a role of space between inner and outer nanotubes. Figure 4 shows the difference between the charge density of the DWNT and the sum of the charge densities of the isolated inner and outer nanotubes, $\Delta\rho = \rho_{(7,0)@(n,0)} - (\rho_{(7,0)} + \rho_{(n,0)})$. It is clear that the electrons are transferred mainly from the π orbitals of both inner and outer nanotubes to the spacious region between the tubes. The amount of the decreased electrons at each atomic site is almost identical so that the total amount of the decreased electrons for the outer nanotube is larger than that of the inner (7, 0) nanotube owing to a site number imbalance between the outer and inner nanotubes. On the other hand, the accumulated electrons are mainly distributed in the interwall region where the atoms are absent.

It is also found that the amount of the accumulated charge decreases with increasing the interwall spacing (Fig. 4). The distribution of the accumulated charge is

TABLE I. The band overlap (E_o) between the π and π^* states for (7, 0)@(16, 0), (7, 0)@(17, 0), (7, 0)@(19, 0), and (7, 0)@(20, 0). The amount of the E_o is defined as $E_o = E_\pi^{\mathrm{KS}} - E_{\pi^*}^{\mathrm{KS}}$, where the $E_{\pi^*}^{\mathrm{KS}}$ and E_π^{KS} are the Kohn-Sham energy levels of the bottom and the top of the π^* and π electron states, respectively. The curvature of each nanotube, $1/r$, is also listed.

Outer tube	E_o (eV)	$1/r$ (1/Å)
(16, 0)	0.00	0.160
(17, 0)	0.13	0.150
(19, 0)	0.12	0.134
(20, 0)	0.13	0.128

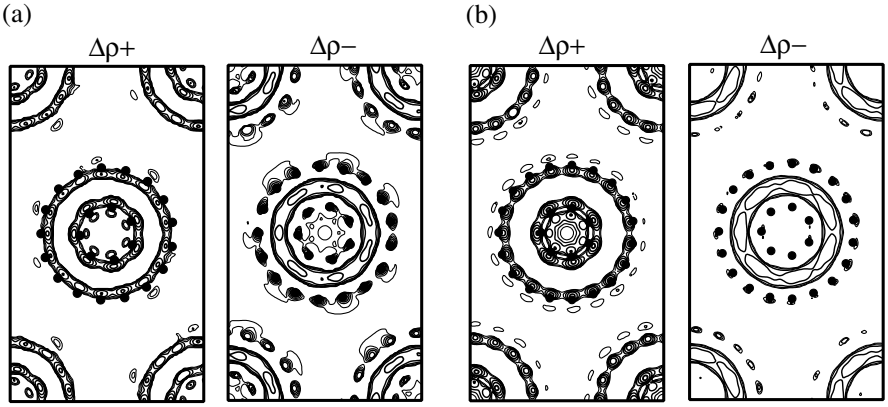

FIG. 4. The contour plots of the more negatively charged (electron rich) area, $\Delta\rho^-$, and that of the more positively charged, $\Delta\rho^+$, than a simple sum of the charge densities of the isolated constituent single-walled nanotubes for (a) (7, 0)@(17, 0) and (b) (7, 0)@(19, 0). Each contour represents twice (or half) of the density of the adjacent contour lines. The lowest values represented by the contour is $4.6875 \times 10^{-3}\ e/(\text{a.u.})^3$.

similar to that of the nearly free electron (NFE) states of the carbon nanotubes, which are the common characteristics of the tubular [26,27] and layered materials [28,29]. The distribution gives evidence of the hybridization between π states of the nanotube and the NFE state. It is noteworthy that the NFE states are still located above E_F by about 2 eV or more and that the distribution shown in Fig. 4 is not the NFE states themselves. The electron states of the DWNTs depend not only on the curvature of the constituent nanotubes but also on the interwall spacing.

The results indicate that the DWNTs with thin innermost nanotubes have the potentiality of a possible application for electron devices. The DWNTs exhibit interesting conduction properties due to the existence of electrons and holes which are distributed on the inner and outer nanotubes, respectively: This may cause a new scheme of controlling the Hall conductivity. On the other hand, by peeling a part of the outer nanotubes [30], we obtain the DWNT with a partly single-walled structure. In this case, the nanotubes possess metal-insulator borders at the edges of the outer nanotube. Thus, it is expected that the border may be applicable for a diode in the nanometer-scale electronic circuit.

We benefited from fruitful conversations with K. Hirahara. This work was partly supported by ACT-JST, Special Research Project on Nanoscience in University of Tsukuba, NEDO under the Nanotechnology Materials Program, and Grant-in-Aid for Scientific Research. Computations were done at ISSP, University of Tokyo, at SIPC, University of Tsukuba, and at RCCS, Okazaki National Institute.

[1] S. Iijima, Nature (London) **354**, 56 (1991).
[2] S. J. Tans, A. R. M. Verschueren, and C. Dekker, Nature (London) **393**, 49 (1998).
[3] N. Hamada, S. Sawada, and A. Oshiyama, Phys. Rev. Lett. **68**, 1579 (1992).
[4] R. Saito *et al.*, Appl. Phys. Lett. **60**, 2204 (1992).
[5] X. Blase *et al.*, Phys. Rev. Lett. **72**, 1878 (1994).
[6] Z. M. Li *et al.*, Phys. Rev. Lett. **87**, 127401 (2001).
[7] Y. Miyamoto, S. Saito, and D. Tománek, Phys. Rev. B **65**, 041402 (2001).
[8] A. Thess *et al.*, Science **273**, 483 (1996).
[9] P. Delaney *et al.*, Nature (London) **391**, 466 (1998).
[10] Y.-K. Kwon, S. Saito, and D. Tománek, Phys. Rev. B **58**, R13314 (1998).
[11] L. F. Sun *et al.*, Nature (London) **403**, 384 (2000).
[12] L.-C. Qin *et al.*, Nature (London) **408**, 50 (2000).
[13] B.W. Smith, M. Monthioux, and D. E. Luzzi, Nature (London) **396**, 323 (1998).
[14] J. Sloan *et al.*, Chem. Phys. Lett. **316**, 191 (2000).
[15] P. Hohenberg and W. Kohn, Phys. Rev. **136**, B864 (1964).
[16] W. Kohn and L. J. Sham, Phys. Rev. **140**, A1133 (1965).
[17] J. P. Perdew and A. Zunger, Phys. Rev. B **23**, 5048 (1981).
[18] D. M. Ceperley and B. J. Alder, Phys. Rev. Lett. **45**, 566 (1980).
[19] N. Troullier and J. L. Martins, Phys. Rev. B **43**, 1993 (1991).
[20] L. Kleinman and D. M. Bylander, Phys. Rev. Lett. **48**, 1425 (1982).
[21] S. Okada, S. Saito, and A. Oshiyama, Phys. Rev. Lett. **86**, 3835 (2001).
[22] O. Sugino and A. Oshiyama, Phys. Rev. Lett. **68**, 1858 (1992).
[23] K. Hirahara (unpublished).
[24] K. Hirahara *et al.*, in *Proceedings of the 15th International Congress on Electron Microscopy (ICEM15), Durban, South Africa, 2002*, edited by J. A. A. Engelbrecht (Microscopy Society of Southern Africa, Onderstepoort, South Africa, 2002), Vol. 1, p. 243.
[25] T. Miyake and S. Saito (unpublished).
[26] Y. Miyamoto *et al.*, Phys. Rev. Lett. **74**, 2993 (1995).
[27] S. Okada, A. Oshiyama, and S. Saito, Phys. Rev. B **62**, 7634 (2000).
[28] M. Posternak *et al.*, Phys. Rev. Lett. **50**, 761 (1983).
[29] M. Posternak *et al.*, Phys. Rev. Lett. **52**, 863 (1984).
[30] J. Cumings, P. G. Collins, and A. Zettl, Nature (London) **406**, 586 (2000).